# Plasmonic enhancement of one-photon- and two-photon-excited single-molecule fluorescence by single gold nanorods

Zhang, W.

# 5

# Plasmonic enhancement of two-photon-excited luminescence of single quantum dots by individual gold nanorods

*Plasmonic enhancement of two-photon-excited fluorescence is not only of fundamental interest but also appealing for many bioimaging and photonic applications. The high peak intensity required for two-photon excitation may cause shape changes in plasmonic nanostructures, as well as transient plasmon broadening. Yet, in this work, we report on strong enhancement of the two-photon excited photoluminescence of single colloidal quantum dots close to isolated chemically synthesized gold nanorods. Upon resonant excitation of the localized surface plasmon resonance, a gold nanorod can enhance the photoluminescence of a single quantum dot more than* $10,000$*-fold. This strong enhancement arises from the combined effect of local field amplification and the competition between radiative and nonradiative decay rate enhancements, as is confirmed by time-resolved fluorescence measurements and numerical simulations.*

## 5.1. Introduction

Due to their unique properties associated with surface plasmons, nanostructures based on metal nanoparticles have been extensively studied for their potential in various applications, such as surface-enhanced Raman spectroscopy [1, 2], metal-enhanced fluorescence [3–5] and second harmonic generation [6, 7]. Plasmonic nanostructures were found to significantly enhance the fluorescence emission of adjacent chromophores as a result of the interplay of several factors, including excitation enhancement because of the high local field, spontaneous radiative emission enhancement from resonant Purcell effect and fluorescence quenching due to nonradiative energy transfer to the metal [8, 9].

Apart from the extensive research on the enhancement of conventional one-photon-excited fluorescence [3, 10–13], the last two decades have seen a growing interest in metal-enhanced fluorescence under two-photon excitation, which is known for the advantages of intrinsic optical sectioning, deeper penetration into biological tissues and, under certain conditions, lower photo-damage. Upon two-photon excitation, a much larger fluorescence enhancement is expected because of the quadratic dependence of two-photon absorption on the excitation intensity. Starting from the 1990s, metal-enhanced two-photon-excited fluorescence has been experimentally demonstrated with lithographically made flat or patterned metal films [9, 14, 15]. There have been also reports on the enhancement of upconversion luminescence using plasmonic nanoparticles [16, 17].



Wet-chemically synthesized metal nanoparticles have been exploited as important alternative structures for plasmonic enhancement [8, 10, 18, 19]. Among many types of metallic nanoparticles, gold nanorods are the most extensively explored. Their intense electromagnetic fields associated with the narrow, strong and tunable plasmon resonance contribute to large enhancement of the fluorescence signal of nearby fluorescent emitters such as molecules and quantum dots. Compared to metal surfaces and nanoparticle clusters [20, 21], individual gold nanorods open the study of plasmon-choromophore interactions in a more reproducible and controllable way owing to their well-defined single-crystalline structure. Compared to nanogap antennas, such as bow-ties, dimers or particles on mirror, nanorods present a more open near field, which can accommodate molecules of various sizes. Moreover, gold nanorods are chemically inert and biocompatible, therefore they are particularly interesting for biotechnological applications.

A few recent reports have successfully demonstrated enhanced two-photon absorption and emission using various systems of nanocomposites composed of colloidal nanorods surrounded by fluorophores [9, 22–25]. However, the enhancement factors reported in ensembles are reduced by averaging over many fluorophores, most of which are not in the best position.

Combined single-molecule and single-particle measurements are needed to bridge the gap between theory and experiments. Moreover, single-molecule and single-particle measurements have the potential of revealing the intrinsic nature of the plasmon-emitter interactions that is usually hidden in ensemble experiments by nanoparticle inhomogeneities, such as size fluctuations and local environment variations.

While seemingly a straightforward idea, two-photon-excited fluorescence enhancement with a single-emitter-single-nanostructure system was investigated theoretically [26] and only achieved experimentally in a very recent work by Gong *et al.*, where the two-photon

excited luminescence intensity from single epitaxially grown InGaN quantum dots (QDs) was enhanced by a factor of 5000 using the strong field enhancement by a silver-coated pyramid structure at a temperature of 7 K [27]. Indeed, two possible major obstacles stand in the way to experimentally testing the two-photon fluorescence enhancement. First, the high peak intensities required for efficient two-photon excitation might damage the plasmonic structure, if not after a single pulse, certainly upon repeated excitation by millions of pulses over long acquisition times. Photothermal reshaping of gold nanorods under femtosecond pulses [28–30] limits the laser intensity one can use for two-photon excitation. Second, the excitation by intense femtosecond pulses tremendously heats up the electron gas by up to thousands of K, thereby broadening the plasmon resonance [31] and potentially hindering plasmonic enhancement. Added to the difficulty of a precise positioning of a single emitter with respect to the near field of plasmonic structures, these two problems may hamper plasmonic enhancement of two-photon excitation.

Our earlier studies have shown that, by exploiting the random diffusion of single molecules around single gold nanorods, the fluorescence of a low-quantum-yield dye could transiently be enhanced by three orders of magnitude [8, 18]. Motivated by the theoretical limit to two-photon-excited fluorescence enhancement, we exploited diffusion and transient sticking of single colloidal QDs to study the strong enhancement of their two-photon-excited luminescence by single gold nanorods at room temperature. We find enhancement of two-photon-excited luminescence by more than four orders of magnitude for *single* QDs in the vicinity of a *single* immobilized gold nanorod at room temperature. The enhancement factor shows a clear dependence on the nanorod's surface plasmon resonance wavelength and is maximum when the resonance wavelength overlaps with the excitation laser wavelength. The achieved enhancement is in good agreement with the predictions of numerical calculations. The dependence on surface plasmon resonance (SPR) wavelength and the fair agreement with simulations show that the transient broadening of the plasmonic resonance by femtosecond excitation is not a limiting factor for two-photon-excited fluorescence enhancement by individual gold nanorods.



## 5.2. Materials and methods

**Gold nanorods**. Aqueous suspensions of cetyltrimethylammonium bromide (CTAB) stabilized gold nanorods were purchased from Nanopartz Inc. (A12-40-780-CTAB). The average size was 38 nm $\times$ 118 nm by diameter and length. Individual isolated gold nanorods were immobilized onto a glass coverslip by spin coating suspensions with reduced CTAB concentration [18]. After spin coating we removed the stabilization ligands from the surface of the gold nanorods by ozone treatment for 30 minutes. This results in bare gold nanorods (*i.e.* without any ligands on their surface), allowing easy access for the quantum dots.

**Two-photon microscopy**. We performed two-photon excited luminescescence measurements on a home-built sample-scanning fluorescence microscope system similar to Chapter 4. The glass coverslip with deposited gold nanorods was immersed in a dilute aqueous solution of QDs. A mode-locked titanium-sapphire laser (Coherent Mira 900) was used as the two-photon excitation source, operating at 775 nm, 76 MHz pulse repetition rate and $\sim$ 220 fs pulse width. The excitation power was measured at the output of the objective. Circular polarization was used, as it excites all the GNRs irrespective of their random orientation in

the focal plane. Time-resolved photoluminescence photons from QDs and gold nanorods were passed through a 650-nm bandpass filter (HQ650/50, Chroma) and recorded with an avalanche photodiode (APD) and processed with a time-correlated single photon counting (TCSPC) card (TimeHarp 200, PicoQuant GmbH). The bandpass filter was used to pass through the luminescence from QDs while reducing the background from two-photon photoluminescence of nanorods. A 532-nm continuous wave laser and a spectrometer equipped with a liquid-nitrogen-cooled CCD (Acton SP-500i, Princeton Instruments) were used to measure the one-photon-excited luminescence spectrum of each nanorod, which was shown previously [32] to closely resemble its scattering spectrum. Spectra of nanorods were measured in water without QDs prior to the enhancement measurements. The spectra were corrected for the spectral response of the optical setup and instruments. Only single nanorods evidenced by their narrow Lorentzian spectral lineshapes were considered in this study. See Chapter 4 for a more detailed description of the optical setup and spectral correction.

## 5.3. Results and discussion



The colloidal QDs in our study (Qdot 655 ITK amino (PEG) from Invitrogen) are CdSe/ZnS core-shell structures, which are further coated with an amphiphilic polymer shell to enable conjugation of amine-derivatized polyethylene glycol. Their overall shape is rod-like and the length and width are $\sim$ 12 nm and $\sim$ 7 nm, respectively [33]. See Supporting Information for more details about the QDs structure. The narrow emission band centered at 655 nm is well away from the longitudinal plasmon resonance of the gold nanorods as can be appreciated in Fig. 5.1. This feature results in a good contrast of signal from single quantum dots against a background from the intrinsic luminescence of the gold nanorods if an appropriate bandpass filter is used. Two-photon photoluminescence was excited by a mode-locked titanium-sapphire laser operating at 76 MHz pulse repetition rate and $\sim$ 220 fs pulse width. The wavelength was set to 775 nm to efficiently excite the longitudinal plasmon resonance of the gold nanorods.

To determine whether the photoluminescence of QDs generated by the femtosecond laser is a result of instantaneous two-photon absorption, we measured the photoluminescence emission intensity from a diluted aqueous suspension of Qdot 655 with respect to the average intensity at the center of the focused excitation beam. Figure 5.1(b) plots this relation in log-log scale, yielding a slope of $2.11 \pm 0.03$, which confirms the two-photon excitation origin of the observed luminescence from the QDs.

Prior to the luminescence enhancement experiments, we measured the one-photon-excited photoluminescence spectra of gold nanorods immobilized on a coverslip and immersed in water. We selected single gold nanorods through their narrow and Lorentzian spectral shape for our later measurements. Afterwards, the nanorods were immersed in a 30 nM Qdot 655 solution with 3 mM NaCl (inset of Fig. 5.1(a)). Photoluminescence photons were recorded on individual gold nanorods under the excitation of the femtosecond laser with an average excitation intensity of 1.55 kW/cm$^2$ (1 $\mu$W at the objective focus) at the center of the focused excitation volume. We note that this intensity is well below that required for photothermal reshaping of single gold nanorod with a low number ($\sim$ 1 to $10^4$) of ultrafast pulses [28–30]. Indeed, we did not observe any luminescence intensity change from the gold nanorods upon femtosecond irradiation, even after our extended measurements of several minutes. More-

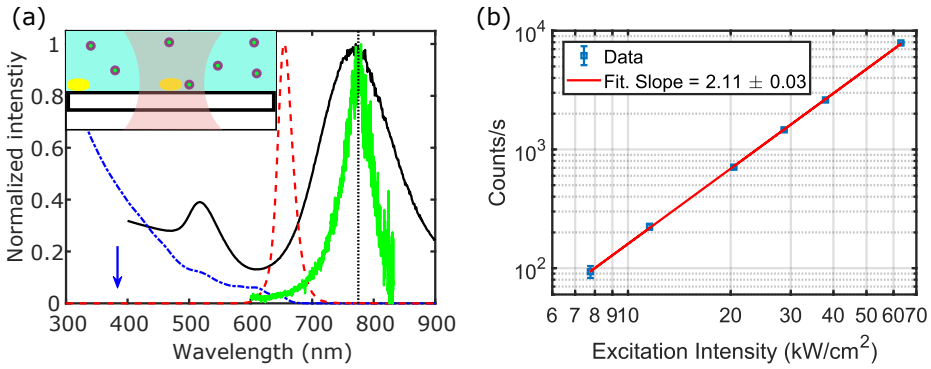


Figure 5.1: **Quantum dots and gold nanorods optical characterization**. (a) Spectra of gold nanorods and quantum dots. The black and green solid lines show the bulk extinction spectrum of gold nanorods dispersed in water and the one-photon-excited photoluminescence spectrum of an immobilized single gold nanorod, respectively. One-photon absorption and emission spectra of the quantum dots diluted in water are shown as the blue dot-dashed line and red dashed lines, respectively. The vertical dotted line shows the wavelength of the Ti:Sapphire laser. The blue vertical arrow indicates the wavelength corresponding to the total energy of two excitation photons. The inset shows a simplified schematics of the enhancement experiment (the yellow cylinders represent gold nanorods; core/shell circles, quantum dots). (b) Log-log plot showing the quadratic dependence of photoluminescence emission of the quantum dots on the excitation intensity. The photoluminescence emission is from a 30 nM quantum dot solution with 1 mM NaCl.



over, the measured one-photon-excited photoluminescence spectra of gold nanorods before and after femtosecond irradiation showed no noticeable changes. Therefore, the nanorods were not reshaped during our measurements. It is worth mentioning that most previous studies on ultrafast reshaping of gold nanoparticles were done with single or a few pulses. Under continuous irradiation of pulses, however, accumulative heating leads to a much lower reshaping threshold in terms of average power. Indeed, we started to observe reshaping for some nanorods with an excitation power $\geq 3\,\mu$W (intensity of $4.7$ kW/cm$^2$ with circular polarization).

Figure 5.2 shows two typical intensity traces (binned to 100 ms) from two gold nanorods whose spectra are shown in the right panels. The spectra have been corrected for the spectral response of the optical setup (see Fig. S2.2 in Chapter 2). Intensity bursts are observed for both nanorods, which we attribute to gold nanorod-enhanced photoluminescence emission of single QDs. Some weak background signal comes mostly from the two-photon-excited luminescence of the gold nanorods [34] (see Fig. S4.6 in Chapter 4). Note that the bursts shown in Fig. 5.2 last generally a few tens of milliseconds to a few seconds.

We used two-photon-excited fluorescence correlation spectroscopy with a two-fold purpose. First, to obtain the diffusion time of our QDs in the confocal volume and second, to measure the single-QD brightness, needed to quantify the enhancement factor.

The diffusion time of a single QD in the near field of a rod is shorter than one microsecond, estimated from the diffusion time in the confocal volume, measured by autocorrelating the two-photon-excited luminescence of freely difussing QDs (Fig. S5.1). Thus we attribute the bursts to transient sticking of QDs onto the substrate and/or the gold nanorods (note that the emitting part of a QD is separated from the gold surface by the polymer coating, therefore

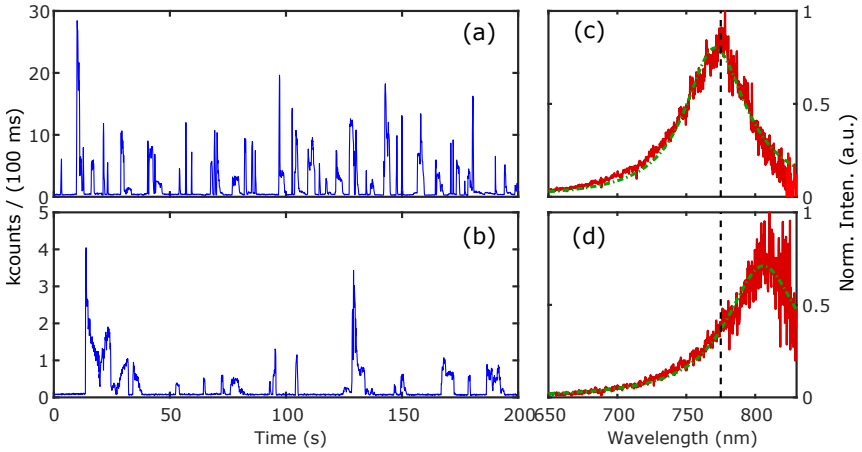


Figure 5.2: **Enhanced two-photon excited luminescence from single QDs.** (a,b) Two-photon-excited luminescence intensity timetraces (100 ms/bin) taken on two single nanorods immersed in 30 nM QD aqueous solution with 3 mM NaCl and (c,d) the corresponding one-photon-excited luminescence spectra of the nanorods measured in water. The excitation intensity at the center of two-photon excitation volume was 1.55 kW/cm$^2$ (circularly polarized). The one-photon-excited spectra show narrow Lorentzian lineshape (green dashed lines), confirming that they are from single nanorods. The low near-infrared response of the optics including the spectrometer CCD is responsible for the high noise. The wavelength of the laser (775 nm) is also shown as the dashed vertical lines in (c) and (d).

sticking to a gold nanorod does not necessarily completely quench its photoluminescence). This nonspecific sticking effect was found in a few studies to be strongly dependent on the properties of the diffuser and the surrounding medium as well as the surface conditions of the metal and substrate [18, 35, 36]. In our case, the addition of a proper amount of NaCl to the QD solution was essential for transient sticking and, hence, for observing luminescence bursts. If no NaCl was added we saw only luminescence from gold nanorods . On the other hand, when the NaCl concentration was too high, the bursts were too long to be separated from each other (data shown in Supporting Information Fig. S5.5).

From the correlation measurements explained in detail in the Supporting Information, we obtained an average unenhanced single-QD brightness of 1900 $\pm$ 70 counts/s at 15.5 kW/cm$^2$ illumination intensity. We note here that this is an ensemble-averaged result that may show significant fluctuations when compared to single-QD data due to variations from dot to dot, for example in size. We also note that the intensity used for this unenhanced measurement is $\times$ 10 higher than the intensity used for the enhancement experiment on a nanorod.

We attribute the large difference in burst intensities recorded on the same gold nanorod to the random locations and orientations of the QDs with respect to the gold nanorod. Additionally, the size distribution of the QDs in our sample contributes further to the intensity inhomogeneity of the enhancement bursts. We observed that the more intense the bursts are, the shorter they last, as it can be seen in Fig. 5.2. Indeed we confirmed this behavior by plotting the burst duration as a function of the burst detected intensity for an enhanced time

trace (see Fig. S5.2). In addition, we note that we did not observe characteristic luminescence blinking of QDs [37, 38]. However, blinking may occur either on a time scale shorter than our resolution or at times longer than the burst duration. We note that earlier observations indicate that QD blinking is greatly suppressed when coupled to plasmonic structures [39, 40].

Blank experiments were performed to verify that the bursts are from gold nanorod-enhanced single QDs. We recorded timetraces on a area without a nanorod under the same experimental conditions. We also measured single nanorods with the same excitation but immersed in 3 mM NaCl without QDs. In both cases, we never observed any burst, as shown in the example traces in the Suppporting Information (Fig. S5.3). Moreover, we recorded timetraces on *the same* single gold nanorod in solutions with different concentrations of QD (6 nM and 30 nM) and we found higher occurrence of bursts in the solution with higher QD concentration (Fig. S5.4). It clearly demonstrates the linear dependence of burst frequency on QD concentration.

The previous experiments convinced us that the bursts stem from enhanced two-photon-excited luminescence of single QDs. The size of the QDs is as large as the near-field, so it is unlikely that more than one QD reside in the near field. We have to consider the possibility of aggregates of QDs, as we did find evidence of them (Fig. S5.1) with an occurrence of 20 per 300 s in the confocal volume. However, considering a near-field volume that is $\sim 2000$ times smaller than the confocal volume ($V_{\mathrm{conf}} = 3 \times 10^{-2}$ fL, $V_{\mathrm{NF}} = 1.4 \times 10^{-5}$ fL), the probability of seeing one QD aggregate in the near-field in a measuring time of 300 s is only 1%.

In order to calculate the luminescence enhancement factor, we need to compare the two-photon-excited enhanced intensity with the unenhanced brightness of a single quantum dot (i.e. count rate per dot). The former can be extracted from the time traces in Fig. 5.2 and the latter was obtained using two-photon fluorescence correlation spectroscopy (FCS) [41]. The same QD solution used for the enhancement experiment was excited with an average excitation intensity of 15.5 kW/cm$^2$ (below saturation). By scaling with the quadratic power dependence of two-photon-excited luminescence, we found the count rate per dot to be $19.0 \pm 0.1$ counts/s at an excitation intensity of 1.55 kW/cm$^2$. See the Supporting Information (Fig. S5.1) for details. The maximum intensity of the burst shown in Fig. 5.2(a) is $2.84 \times 10^2$ kcounts/s for circularly polarized excitation. It is from a single QD enhanced by the nanorod against a background signal of 2850 counts/s from the nanorod and other QDs in the focal volume. Based on a brightness of 19.0 counts/s per QD measured with FCS at the same excitation intensity, we calculate an enhancement factor of $1.5 \times 10^4$ for circularly polarized light. We used circularly polarized light to excite all the nanorods in the glass surface, regardless of their orientation. If we would use linearly polarized light parallel to the long axis of the nanorod, we expect to observe a larger enhancement of $6 \times 10^4$.

We would like to emphasize that the reported enhancement factor comes from looking at the highest burst in a time trace, as is commonly done in the literature. However, there are other alternative methods to obtain the enhancement factor from the same type of experimental data, leading to similar results [42].

Comparison of Fig. 5.2(a) and (b) clearly reveals that the enhancement strongly depends on the longitudinal plasmon resonance wavelength of the gold nanorod. The plasmon resonance of the nanorod shown in the upper panels matches the laser wavelength very well,

giving rise to almost one order of magnitude more intense bursts than the other nanorod, whose resonance wavelength is $\sim 30$ nm away from the laser wavelength. We repeated the measurements on 23 different individual nanorods and plotted their maximum luminescence enhancement factors in Fig. 5.3(a). The strongest enhancement was achieved by a nanorod with a surface plasmon resonance wavelength of 771 nm. The time trace and spectrum of this nanorod are those shown in Fig. 5.2(a). We note that our observation of two-photon excited enhanced emission gives evidence that the transient plasmon broadening is not serious limitation to the two-photon enhancement.

To understand the measured luminescence enhancement theoretically, we employed a finite-element method (Comsol Multiphysics) and a boundary element method to model the quantum dot-nanorod system. The photoluminescence emission of an emitter in the vicinity of a gold nanorod is altered through the modification of both the excitation and emission rates, as illustrated by Khatua *et al.* considering a two-level model [8]. For excitation intensities below saturation, we can treat absorption and emission independently. This assumption is justified because the saturation intensity is $\sim 2000$ times higher than the incident laser intensity in our enhancement experiments (Fig. S5.7). Such a high saturation intensity is well above the local field intensity that can be attained by the nanorods used in our study, about 300 times larger than the incident intensity. Therefore, the overall enhancement factor is approximated by the product of excitation enhancement and emission enhancement [8]. See the Supporting Information for the details of the simulations.



In Fig. 5.3(a), along with measured photoluminescence enhancement factors, we plot the calculated overall enhancement factors for point emitters that are 5 nm away from the tip of the nanorod as a function of the plasmon resonance wavelength of the nanorod, while the near-field intensity map of the nanorod with the highest enhancement is shown in Fig. 5.3(b). From this map, it is straightforward to obtain the excitation enhancement as $E_{ex} = (I/I_0)^2$, which is shown in panel (d), left axis as a function of the distance to the tip.

In Fig. 5.3(c) we plot the calculated radiative rate enhancement ($k_{\mathrm{r}}/k_{\mathrm{r}}^0$, blue triangles) and relative additional nonradiative rate ($K_{\mathrm{nr}}/k_{\mathrm{r}}^0$, red circles) of a QD against the distance to the tip of a single nanorod. The size of the nanorod in the calculation was 38 nm $\times$114 nm with a plasmon resonance of 775 nm in water. The high additional nonradiative rate due to the strong absorption of the gold nanorod (quenching) leads to an emission "enhancement" factor that is lower than unity.

The emission enhancement is proportional to the inverse of the emitter's intrinsic quantum yield (see Supporting Information), which is not a priori known in our experiments. First, the quantum yield of individual QDs varies due to the size distribution [33]. Second, it is known that the quantum yield of a single QD fluctuates with time in a manner that is strongly correlated with the luminescence lifetime [43–46]. Moreover, the presence of on-off blinking and intermediate states [44] adds further complications to the "on-state" quantum yield of a QD.

In addition to these unknown parameters of the system, we modeled the measured lifetime decay with three exponential components (see supporting information Fig. S5.6 for details) for unenhanced QDs in solution. The obtained lifetimes are $\tau_1 = 1.5$ ns, $\tau_2 = 16.5$ ns and $\tau_3 = 46.2$ ns. In the absence of detailed information on the QD emission we used two simple models to calculate the emission enhancement. Model 1 assumes that the three components have the same radiative rate $k_{\mathrm{rad}}^0$. We then use the measured lifetimes to obtain

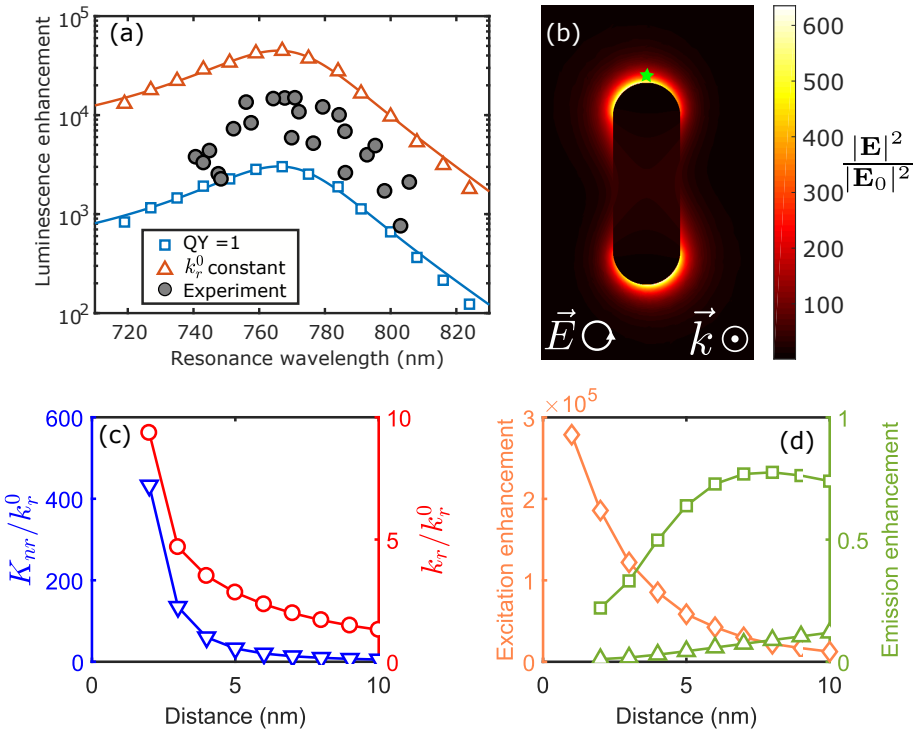


Figure 5.3: **Enhancement dependence with plasmon resonance.**(a) Measured maximum two-photon excited luminescence enhancement factors for 23 gold nanorods plotted against their plasmon resonance wavelengths are shown as gray circles. The numerically calculated overall enhancement factors for two different models of QD luminescence (see main text) in red triangles and blue squares. Solid lines are guides to the eye. For the calculations, the emitter is assumed to be located 5 nm away from the tip of the nanorod (green star in (b)). (b) Calculated near-field intensity map of a 38 nm $\times$114 nm nanorod in water, with SPR at 775 nm. (c) Calculated radiative rate enhancement ($k_\mathrm{r}/k_\mathrm{r}^0$, red circles, right axis) and relative additional nonradiative rate ($K_\mathrm{nr}/k_\mathrm{r}^0$, blue triangles, left axis) of a QD as a function of the distance to the tip of the nanorod. (d) Calculated excitation enhancement (orange diamonds) and emission enhancement (green squares and triangles) as functions of the distance to the tip of the nanorod. The squares and triangles correspond to the two models mentioned above for (a). The excitation wavelength was 775 nm (circularly polarized) for both experiments and simulations.

the quantum yield for each component. We additionally assumed a unity quantum yield for the longest component. Model 2 assumes unity quantum yield for all three components. In both cases we calculated the emission enhancement for each component individually and then averaged the results with the weights obtained from the lifetime fit shown in the supplementary material. The results for the two models are plotted in Fig. 5.3(a) as a function of the SPR (model 1 as red triangles and model 2 as blue squares) and Fig. 5.3(d) as a function of the gold nanorod-QD distance (model 1 as triangles and model 2 as squares). From Fig. 5.3(a) we see that these two extreme models reproduce the resonance wavelength dependence quite well. The experimental points lay between the two curves, showing that these simple models do not give a complete quantitative description of the system. Figure 5.3(d) shows the calculated two-photon excitation enhancement and emission enhancement as functions of the distance to the tip of the nanorod. Overall, our experimental results agree well with theoretical calculations both for the enhancement factors and the dependence on the resonance wavelength. Therefore, comparison to theory indicates that transient plasmon broadening, if at all present, does not significantly reduce the two-photon-excited fluorescence enhancement.



It is also of interest to investigate the impact of gold nanorods on the photoluminescence lifetime of QDs. The intrinsic two-photon-excited photoluminescence lifetime of the QDs could not be accurately measured with our current system due to the high repetition rate of the titanium-sapphire laser. We noticed that it was reported that the photoluminescence lifetimes of CdSe quantum dots under one- and two-photon excitations are nearly identical [47]. Therefore, we measured the complete photoluminescece decay of the same QD solution with one-photon excitation by using a pulsed picosecond diode laser (Power Technology, Little Rock) with a repetition rate of 1 MHz and a wavelength of 635 nm, and we obtained a non-exponential decay with an average lifetime of 6.3 ns (See Supporting Information for more explanation and Fig. S5.6 for the curve). In the presence of nanorods, we obtained the lifetimes of the enhanced two-photon-excited luminescence from the recorded time-tagged single-photon data. The instrument response function (IRF) was measured by recording luminescence photons from a nanorod in the same spectral range as the QDs [34]. For each time bin of 100 ms, we recorded a luminescence decay histogram and, after deconvoluting the instrument response function, fitted it with a single-exponential function, and plotted the temporal evolution of the lifetimes (i.e. a lifetime trace) in Fig. 5.4(b). The corresponding photoluminescence intensity trace from the same nanorod is plotted as well in Fig. 5.4(a) for comparison. We observed a shortened lifetime smaller than 2 ns due to the presence of the nanorod.

We also calculated numerically the photoluminescene lifetime for a QD near the gold nanorod for the three components using the simple model mentioned before. Figure 5.4(c)-(d) show the expected lifetime for each component and the weighted average result for the two models presented before. In both cases, the weighted average lifetime for a QD in the vicinity of the gold nanorods is below 5 ns, in agreement with the observed shortened lifetime. This strong shortening of lifetime is a combination of an enhanced radiative decay rate ($k_{\mathrm{r}}$) and the additional non-radiative decay pathways due to the dissipation of gold ($k_{\mathrm{nr}}$). The relation between luminescence intensity and lifetime is complicated due to the interplay between electromagnetic intensity enhancement and changes of radiative and nonradiative decay rates.

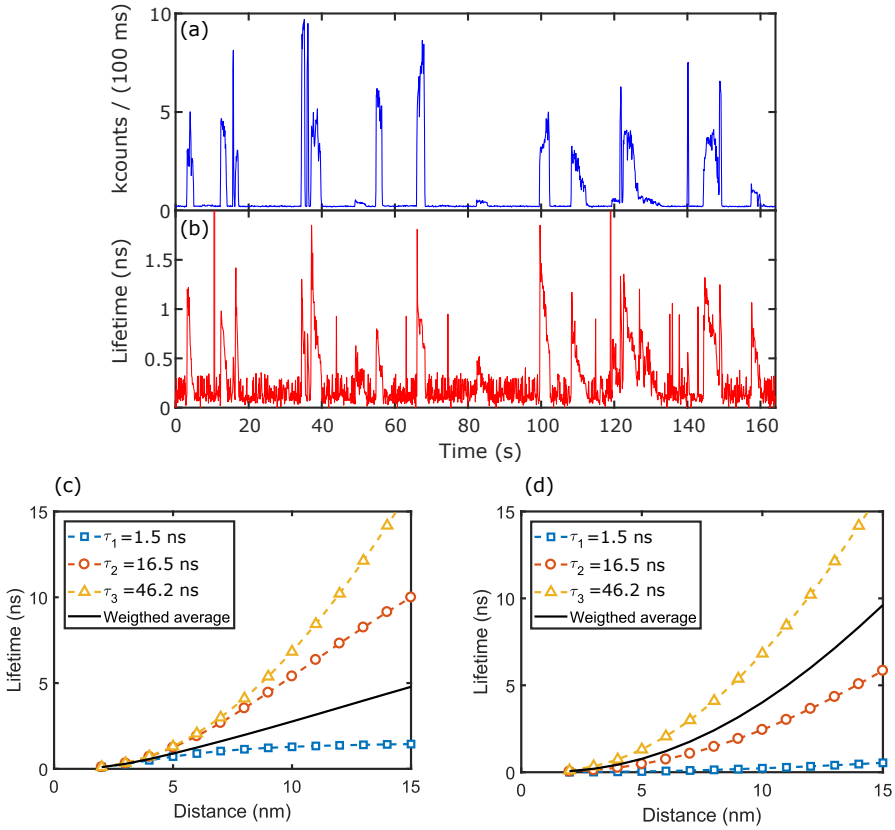


Figure 5.4: **QDs enhanced photoluminescence lifetime.** (a) Photoluminescence intensity trace and the corresponding lifetime trace (b) measured on a single gold nanorod. (c), (d) Calculated lifetime of a QD as a function of the distance to the tip of the nanorod, with different lifetimes indicated in the legend. For the calculation, the size of the single nanorod is 38 nm $\times$114 nm with a plasmon resonance of 775 nm in water, corresponding to the maximum enhancement. For (c) we assumed a constant radiative rate for all the species with a unity quantum yield for the longest component ($\tau_3$). For (d) we assumed unit quantum yield for all the species.

Interestingly, we systematically found many photoluminescence bursts which show nearly constant or even increasing intensities but shorter lifetimes. We speculate that this interesting behavior may be a result of some photochemistry that is happening to the QDs in the vicinity of the nanorods. Oxidation of the QDs is unlikely the cause, as we observed the same phenomenon after removing oxygen by saturating the sample solution with Argon gas (data not shown). With the current set of data and experimental design, we are not able to identify the underlying mechanism. Obviously, the emission intensity and decay rates are strongly dependent on the QD location with respect to the nanorod, which is not a priori known in our case. Further investigations, preferably single-emitter and single-particle studies with well-defined structures and positions, are required to clarify this point.

## 5.4. Conclusions

In summary, this work demonstrates the enhancement of two-photon-excited luminescence from single emitters by wet-chemically synthesized single gold nanorods. Quantum dots with high two-photon brightness are used to detect enough luminescence signal while maintaining the shape of gold nanorods by using very low excitation intensity. An enhancement factor of $15,000$ ($60,000$ with linearly polarized light parallel to the long direction of the nanorod) is achieved by matching the plasmon resonance of gold nanorod with the excitation wavelength. This large enhancement results from the plasmon resonance-enhanced strong near-field at the tips of the gold nanorods and the quadratic dependence of two-photon absorption and the excitation intensity. We also observed a significant change in the quantum dot's luminescence lifetime due to interaction with the nanorods.

The good agreement between our experimental and simulation results suggest that luminescence enhancement is not notably affected by the plasmon broadening due to the presence of high electronic temperatures. We believe this study sheds some light on metal-enhanced fluorescence and paves the way for future studies of single-molecule-single-particle plasmonic enhancement of two-photon-excited luminescence. The luminescence enhancement by gold nanorods will be valuable for two-photon fluorescence applications [9, 23], especially when a low excitation power is required by experimental conditions.

## 5.5. Supporting information

### 5.5.1. Two-photon fluorescence correlation spectroscopy

To measure the average brightness of individual QDs without enhancement, we excite a solution of 30 nM QDs with 3 mM NaCl with fs laser (average $15.5$ kW/cm$^2$, circularly polarized). About 20 high bursts in $300$ seconds can be observed (Fig. S5.1(a)), which cannot be explained by the intensity fluctuations due to single quantum dots diffusing in and out of the focal volume. They are probably a consequence of a small amount of large clusters of QDs present in the solution. The longer time component ($\sim 30$ ms) in the autocorrelation curve for the entire timetrace (back triangles in Fig. S5.1(b)) is probably from the clusters, which diffuse slower than single QDs. We tried several separating and filtering methods to get rid of the clusters, but it appeared that these clusters always reform in the aqueous solution. By autocorrelating photons within a period of time without high bursts (marked

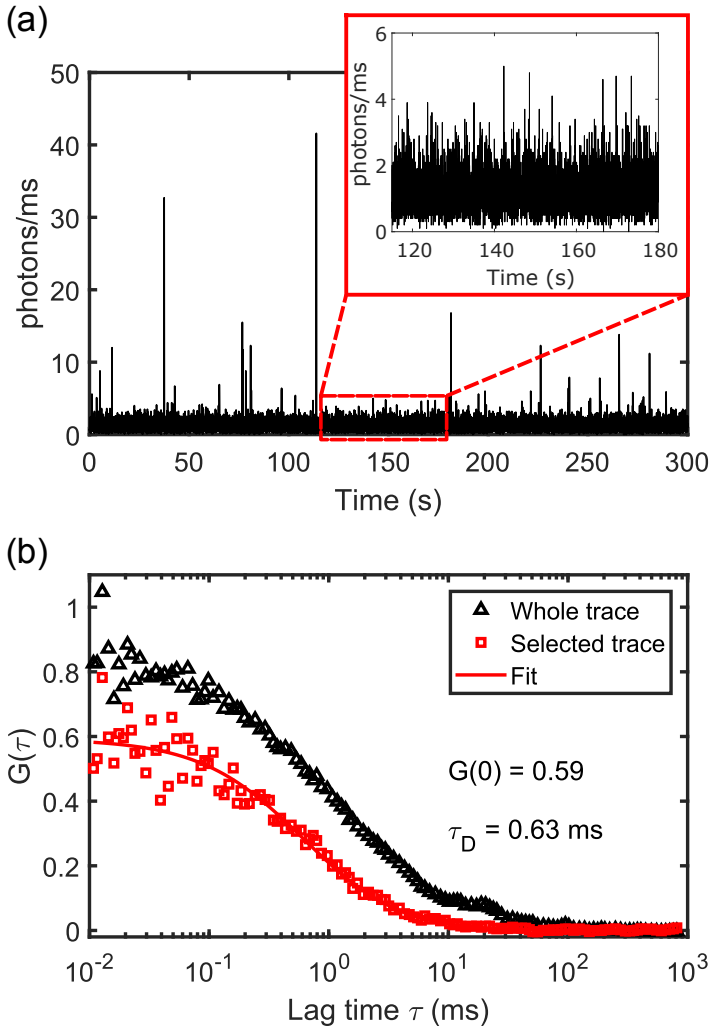


Figure S5.1: (a) Emission intensity time trace (binned to 10 ms) recorded from a solution of 30 nM QDs ($\lambda_{\mathrm{em}} = 655$ nm) with 3 mM NaCl without gold nanorods. The high bursts evidence the presence of aggregates of QDs in the solution. The average excitation intensity was 15.5 kW/cm$^2$. The inset shows a zoom in of the zone marked with the rectangle. This evidences the presence of single-QD bursts. (b) The black triangles plot the autocorrelation curve of the whole timetrace shown in (a). The stretched longer component at $\sim$ 30 ms comes from the strong bursts in (a). The red squares show the autocorrelation for the photons within the marked window in (a). No strong bursts were present in this period of timetrace. The autocorrelation curve can be fitted with a translational diffusion model, yielding an amplitude of $0.59 \pm 0.02$ and a diffusion time $\tau_D$ of $(0.63 \pm 0.07)$ ms.

by a red box in Fig. S5.1(a)), we got the autocorrelation curve for single quantum dots, which is shown as red triangles in Fig. S5.1(b). The autocorrelation curve was fitted with the following diffusion model [48, 49]

$$G(\tau) = G(0)\frac{1}{1+\tau/\tau_D}\frac{1}{\left[1+(w_0/z_0)^2\tau/\tau_D\right]^2},$$

where $w_0$ and $z_0$ are the $1/e^2$ width along the radial and axial direction of the excitation volume, respectively and $\tau_D$ is the diffusion time. For the fitting we used the values $w_0 = (202 \pm 2)$ nm and $z_0 = 560 \pm 5$ nm ($V_{\text{conf}} = 3 \times 10^{-2}$ fL). The fitting result is shown as a solid red line in Fig. S5.1(b). The number of QDs contributing to the average photoluminescence signal ($1130.7 \pm 28.2$ counts/s) is related to the fitted amplitude of the autocorrelation function ($G(0)$) through $N = \gamma/G(0)$, where $\gamma$ is geometrical factor that accounts for the shape of the excitation profile. For an overfilled objective lens, the excitation profile is a 3D-Gaussian and $\gamma = 2^{-3/2}$ , therefore we obtained $N = 0.60 \pm 0.02$, which means a two-photon-excited confocal volume of ($0.03 \pm 0.01$) fL. Then the brightness of each QD was calculated to be $1895 \pm 72$ counts/s at $15.5$ kW/cm$^2$.

By considering the quadratic emission-intensity relation of two-photon photoluminescence, we found that the average brightness of each QD at the intensity used for the enhancement experiments ($1.55$ kW/cm$^2$ at the center of the excitation volume) should be $19.0 \pm 0.7$ counts/s. The excitation intensity was well below saturation. We found no evidence of blinking on microsecond to millisecond time scales, which is in agreement with previous observations [50, 51]. The study by Yao *et al.* suggests that QDs are still blinking in solution but longer dwell times are needed to detect the blinking [41].

## 5.5.2. Burst analysis: correlation between duration and intensity

We analyzed the two-photon excited enhanced time trace shown in Fig S5.2(a) to extract the burst duration and the intensity of each enhancement event and plotted the burst duration as a function of the intensity observed during the burst. Figure S5.2(b) shows the correlation plot between these two quantities in linear scale and (c) in log-log scale. We see that the high-intensity bursts have a short duration and that bursts with low intensity usually last longer.

## 5.5.3. Blank experiments

We performed some blank experiments to corroborate that the luminescence signal observed was indeed coming from the QDs and not from some other chemical species in the solution. First, we measure under the same experimental conditions used for the enhanced experiment in a position far away from any nanorod. The obtained time trace in this case is shown in Fig. S5.3(a). No bursts are observed. Note that the quantum dots are diffusing during the experiment and that at this extremely low power the two-photon excitation does not provide much signal.

Second, we measured in the same experimental conditions used for the enhancement but in a solution without any QDs on top of a nanorod. The measured time trace for this case is shown in Fig. S5.3(b) with an inset showing the scheme of the experiment. Again, there are

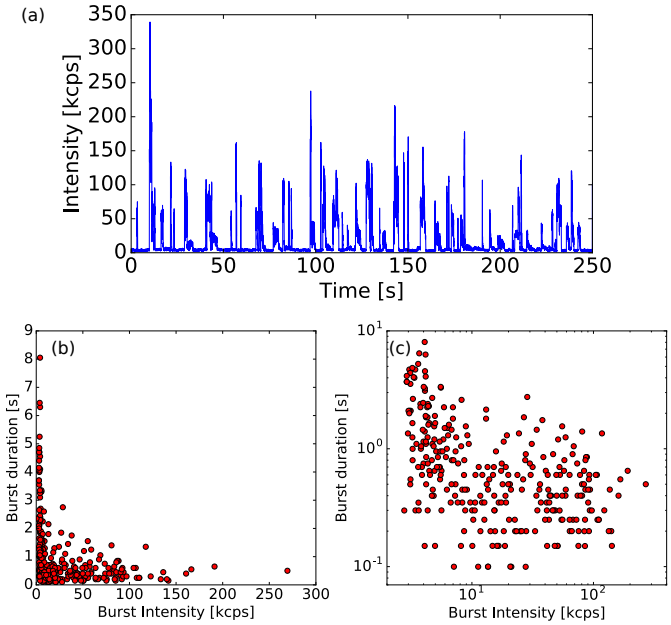


Figure S5.2: (a) Two-photon-excited photoluminescence enhanced time trace of Qdot 655. (b) Linear scale plot of the burst duration as a function of the burst intensity. (c) Same plot as (b) in log-log scale.

not bursts, as expected, but there is a significant contribution that we assign to two-photon excited photoluminescence of the gold nanorods. This is a quite efficient process since the laser is hitting the surface plasmon resonance of the particle and thus the absorption cross section is remarkably high.

## 5.5.4. Quantum dot concentration dependence

We also studied the concentration dependence of the enhanced signal from single QDs. We observed an approximate 5 times increase in the number of events registered in 275 s when we increase the concentration by a factor of 5 (see Fig. S5.4).

## 5.5.5. Enhancement time traces at different NaCl concentration

We took traces at different concentration of NaCl to empirically obtain the optimum concentration for our study. We seek a situation where we have clearly distinguished enhancement events, sparse enough in time to address them individually. Figure S5.5 shows two time traces, the top one at 1 mM and the bottom one at 5 mM concentration of NaCl. We see that when the concentration is too high, the enhancement events overlap in time, complicating the analysis.

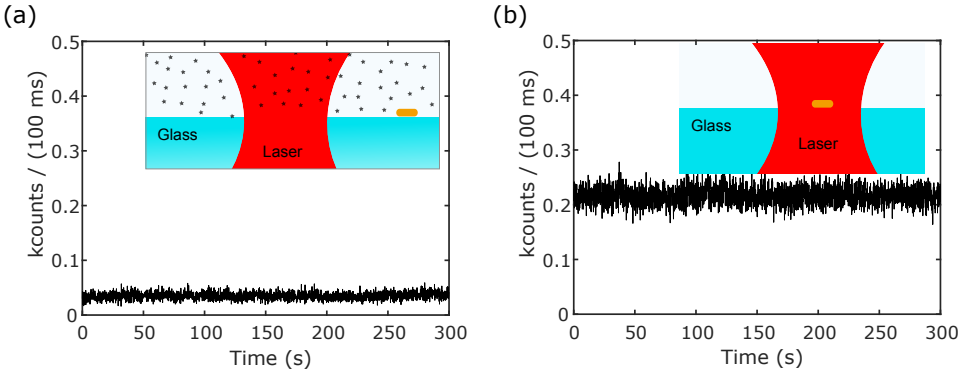


Figure S5.3: (a) A timetrace recorded on a solution of 30 nM QD and 3 mM NaCl in water, with no gold nanorod present. (b) A timetrace taken on a single gold nanorod in 3 mM NaCl, with no QD present. In both experiments, the excitation conditions were the same as in the enhancement experiment (Fig. 5.2 in the main text).

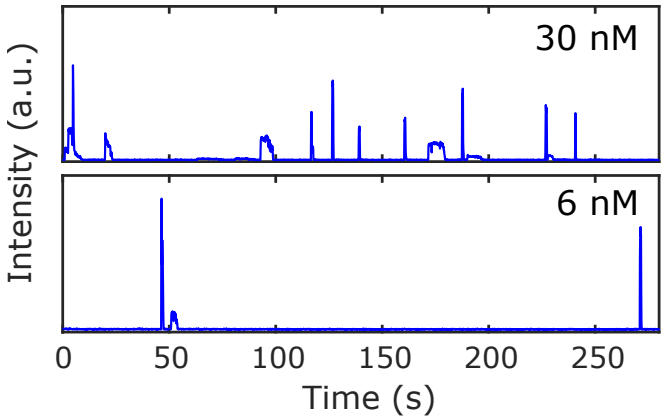


Figure S5.4: Timetraces recorded on the same gold nanorod at two different QD concentrations (6 nM and 30 nM). The timetrace for 30 nM is shifted for clarity. The excitation is 1.55 kW/cm$^2$ at 775 nm.

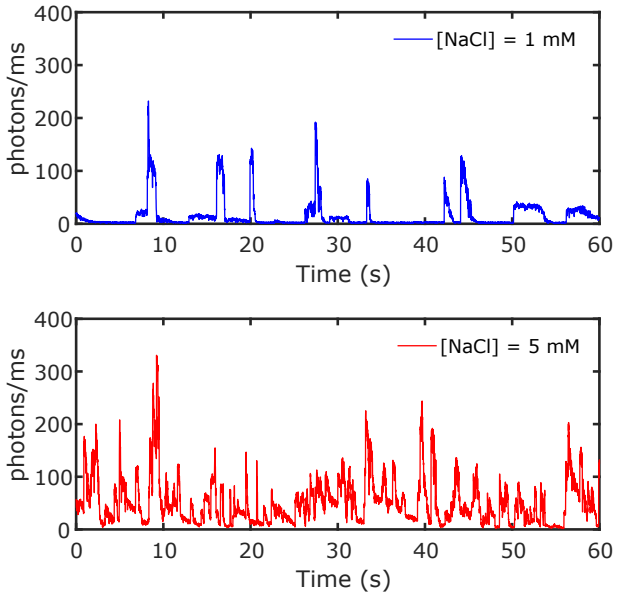


Figure S5.5: Enhanced time traces of QDs by gold nanorods at different concentrations of NaCl. Top 1 mM, bottom 5 mM.



## 5.5.6. One-photon luminescence decay of quantum dots

To measure the complete luminescence decay, an aqueous solution of 150 nM Qdot 655 and 3 mM NaCl was excited by a picosecond diode laser (Power Technology, Little Rock, AR, USA) with a wavelength of 635 nm and a repetition rate of 1 MHz. The emission was detected by an avalanche photodiode (SPCM AQRH-15, Perkin Elmer Inc., USA) and counted by a TCSPC card (PicoHarp 300, PicoQuant GmbH, Berlin, Germany). Figure S5.6 shows at the top the PL decay of the sample over a time window of 1 $\mu$s, along with the impulse response function of our system. We observe a non-exponential decay, commonly reported in the literature for quantum dots and usually attributed to the size distribution [39, 46], blinking and environmental fluctuations [44, 45, 52].

In order to model this behavior we used a stretched exponential [45]

$$f(\tau) = A\exp\Big[\big(-\tau/\tau_0\big)^{\beta}\Big],$$

and, alternatively, three exponentials

$$g(\tau) = w_1 e^{-\tau/\tau_1} + w_2 e^{-\tau/\tau_2} + (1 - w_1 - w_2)e^{-\tau/\tau_3}$$

to fit the decay. We also show both fits in Fig. S5.6. For the stretched exponential we obtained a $\tau_0 = 1.51$ ns and an exponent $\beta = 0.39$, while for the three exponentials we obtained obtaining $\tau_1 = 1.5$ ns ($w_1 = 66.92\%$), $\tau_2 = 16.5$ ns ($w_2 = 25.06\%$), $\tau_3 = 46.2$ ns

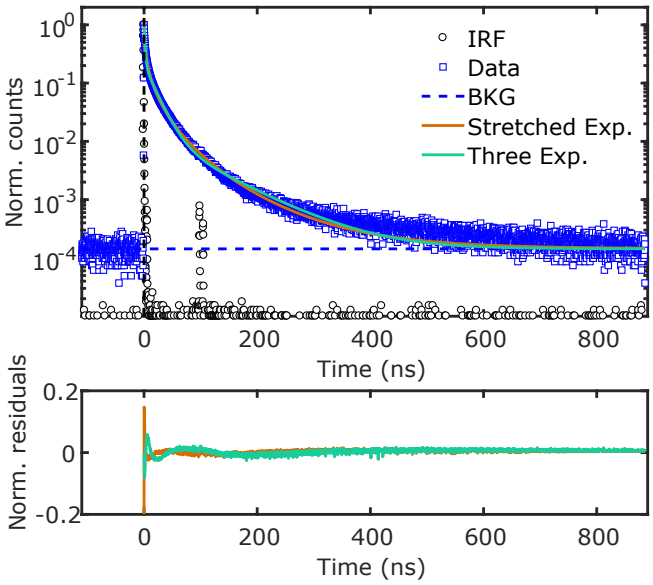


Figure S5.6: One-photon-excited luminescence decay curve of Qdot 655 diluted in water (150 nM). Top: decay data from QDs (blue squares) and IRF (black circles). The vertical dashed line shows $t = 0$ s while the horizontal dashed line represents the background signal. The fits for stretched exponential and three exponentials are also shown. Bottom: residuals from the fits with the same color code used on top.

($w_3 = 8.02\%$). Note that our curves are normalized to get a unity value at zero time and the percentage amplitudes in brackets correspond to the percentage weight of each exponential.

For the stretched exponential model, we calculated the average lifetime by [45]

$$\langle \tau \rangle = \frac{\tau_0}{\beta} \Gamma\left(\frac{1}{\beta}\right) = 5.09 \text{ ns}$$

where $\Gamma$ represents the gamma function.

For the three-exponential model, we calculated different probabilities of the three QD forms according to the two models presented in the main text.

In model 1, the probabilities of the three forms are just proportional to the initial fluorescence intensity $w_i$, because their radiative rate is identical and thus initial intensities are proportional to the number of QDs. Thus we obtained an amplitude-weighted average lifetime of 8.88 ns by

$$\langle \tau_{\text{amp}} \rangle = \sum_i w_i \tau_i.$$

In model 2, because the quantum yield is the same for all three populations of QDs, these populations are proportional to the total number of photons emitted, corresponding to new weights $W_i = w_i \tau_i / \sum_j w_j \tau_j$. We obtained $W_1 = 11.54\%, W_2 = 46.68\%, W_3 = 41.78\%$. Thus we obtained an intensity-weighted average lifetime of 27.22 ns by

$$\langle \tau_{\text{int}} \rangle = \sum_i W_i \tau_i.$$

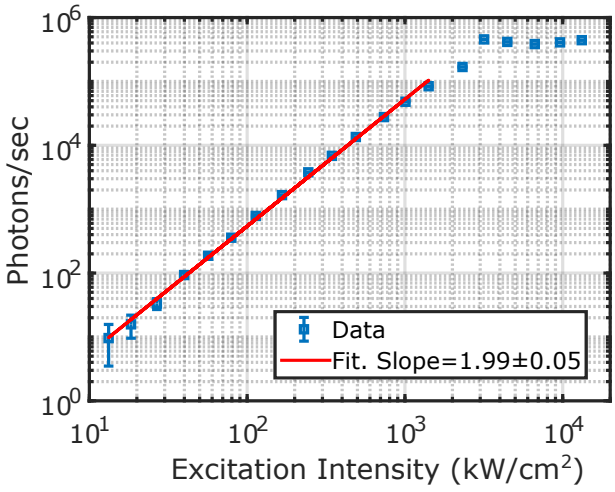


Figure S5.7: Two-photon-excited photoluminescence signal from an aqueous solution of Qdot 655 doped with 3 mM NaCl as a function of the excitation intensity at the center of the focused excitation volume. The curve deviates from the intensity-square relation at high intensities, indicating an excitation saturation threshold of $\sim$ 3000 kW/cm$^2$.



**QDs quantum yield**

We measured the ensemble quantum yield (QY) of the quantum dots using a fluorometer and obtained 0.80 $\pm$ 0.05. The quantum yield $\eta_i$ of each component $i$ is

$$\eta_i = \frac{k_{ri}}{k_{ri} + k_{nri}} = \tau_i k_{ri}$$

where $k_r$ and $k_{nr}$ represents the radiative and non-radiative rates and $\tau_i$ is the lifetime for each component. For model 1, with $\eta_3$ = 1 we can calculate the average quantum yield as

$$\langle \eta \rangle = \sum_i w_i \eta_i,$$

and obtained a value of $\langle \eta \rangle$ = 0.19. For model 2, the average quantum yield is obviously unity. Thus, the two extreme models give upper and lower bounds to the expected experimental values.

## 5.5.7. Excitation saturation

We performed a power dependence study of the collected luminescence of a solution of QD in the same conditions as the enhancement experiment. This time we increased the excitation intensity until we found the saturation value (Fig. S5.7). We find that the saturation occurs at $\sim$ 3000 kW/cm$^2$, which is $\sim$ 2000 times higher than the intensity used for the enhancement experiments.

### 5.5.8. Enhancement factor simulations

The excitation enhancement was calculated with a finite-element method using Comsol Multiphysics. The near-field intensity maps of single gold nanorods with resonance wavelengths ranging from 711 to 824 nm in water were calculated. The resonance wavelengths were tuned by changing the length while keeping a constant diameter of 38 nm. The dielectric permitivity for gold was taken from Johnson and Christy [53], and the refractive index of the ambient medium was taken as 1.33. The theoretical excitation enhancement $E_{\mathrm{exc}}$ for two-photon absorption is the squared ratio of local field intensities with and without the nanorod, $E_{\mathrm{exc}} = I^2/I_0^2$, at the emitter's position.

We used a boundary element method (SCUFF-EM) to evaluate the modifications of decay rates and emission enhancement using a classical electrodynamics approach [54, 55]. For simplicity, a QD was modeled as a radiating point dipole ($\mathbf{p}_0$) oscillating at a frequency of $\omega$, which corresponds to the emission wavelength of the QD.

The time-average power radiated by a QD in a medium is

$$P_{\mathrm{r0}}(\omega) = \frac{|\mathbf{p}_0|^2}{4\pi\varepsilon_0}\frac{n\omega^4}{3c^3},$$

where $n$ is the relative index of the medium, $c$ is the speed of light and $\varepsilon_0$ is the vacuum permittivity. In the vicinity of a nanoantenna, however, both the radiative and nonradiative decay rates are modulated by coupling to the plasmonic modes. The radiative rate enhancement factor ($E_{\mathrm{rad}}$) due to resonant Purcell enhancement can be calculated as the ratio of the total radiated power by the emitter-antenna system ($P_{\mathrm{rad}}$) and the power radiated by an isolated emitter ($P_{\mathrm{r0}}$):

$$E_{\mathrm{rad}} = k_{\mathrm{r}}/k_{\mathrm{r}}^0 = P_{\mathrm{rad}}/P_{\mathrm{r0}},$$

where $k_{\mathrm{r}}$ and $k_{\mathrm{r}}^0$ are the radiative decay rates with and without the antenna, respectively. Likewise, the additional nonradiative rate ($K_{\mathrm{nr}}$) due to the dissipative losses inside the metal is derived from the power absorbed by the nanorod ($P_{\mathrm{abs}}$):

$$K_{\mathrm{nr}}/k_{\mathrm{r}}^0 = P_{\mathrm{abs}}/P_{\mathrm{r0}}.$$

In the simulation, $P_{\mathrm{abs}}$ was calculated by integrating the time-averaged Poynting flux over the nanorod surface, which was modeled as a spherically capped cylinder. The sum of $P_{\mathrm{rad}}$ and $P_{\mathrm{abs}}$ was calculated as [56]

$$P_{\mathrm{rad}}(\omega) + P_{\mathrm{abs}}(\omega) = \frac{\omega^3}{2c^2\varepsilon_0}|\mathbf{p}_0|^2\left[\mathbf{n}\cdot\mathrm{Im}[\mathbf{G}(\mathbf{r},\mathbf{r};\omega)]\cdot\mathbf{n}\right],$$

where $\mathbf{G}(\mathbf{r},\mathbf{r};\omega)$ is the Green tensor at the emitter's position $\mathbf{r}$, $\mathbf{n}$ the unit vector in the direction of the dipole moment. The emission enhancement factor can be written as

$$E_{\mathrm{em}} = \frac{\eta}{\eta_0} = \frac{E_{\mathrm{rad}}}{\eta_0\left(E_{\mathrm{rad}} + K_{\mathrm{nr}}/k_{\mathrm{r}}^0 + 1/\eta_0 - 1\right)} \approx \frac{E_{\mathrm{rad}}}{\eta_0\left(E_{\mathrm{rad}} + K_{\mathrm{nr}}/k_{\mathrm{r}}^0\right)},$$

where $\eta$ and $\eta_0$ are the quantum yield of the emitter with and without the antenna, respectively. $E_{\mathrm{em}}$ is proportional to the inverse of the emitter's intrinsic quantum yield for a given

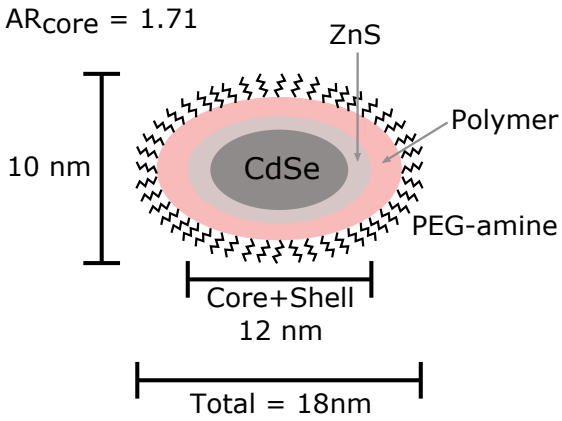


Figure S5.8: Scheme of the QDs used for the study.



emitter-antenna configuration, but independent of its intrinsic lifetime. Due to emission enhancement, the luminescence lifetime of the emitter is shortened:

$$\tau/\tau_0 = \eta_0^{-1}\left(E_{\mathrm{rad}} + K_{\mathrm{nr}}/k_{\mathrm{r}}^0 + 1/\eta_0 - 1\right)^{-1} \approx \eta_0^{-1}\left(E_{\mathrm{rad}} + K_{\mathrm{nr}}/k_{\mathrm{r}}^0\right)^{-1}.$$

In the calculation of $E_{\mathrm{rad}}$ and $K_{\mathrm{nr}}$, it was assumed that the point dipole is placed along the long axis of the nanorod with a certain distance from the tip, and all the results were averaged over the actual luminescence spectrum of the QD. Unlike a fluorescent molecule, an elongated QD has three dipolar axis, where two are degenerated. Therefore, we simulated both orientations, parallel ($\parallel$) and perpendicular ($\perp$) and averaged the results using $1/3(\parallel +2\ \perp)$.

We modeled the three components with lifetimes $\tau_i$ ($i = 1, 2, 3$) independently using the above approach and then averaged the results using the weights $w_i$ obtained from the fit of the natural lifetime decay (Fig. S5.6). We used two extreme models to assign the quantum yield of each component. In model 1 we assume that the radiative rate of all the components is the same and we assigned a unity quantum yield to the longest component. In model 2 we assigned unity quantum yield to the three components.

## 5.5.9. Quantum dot structure

For our study we used commercial quantum dots from Invitrogen (Qdot 655 ITK amino-PEG). They have a core-shell structure of CdSe/ZnS with a rod-like shape. The length and width are 12 nm and 7 nm, respectively, giving an aspect ratio of 1.71. It is further coated with an amphiphilic polymer shell to enable conjugation of amine-derivatized polyethylene glycol (PEG). Figure S5.8 shows a scheme of the QDs. The last layer of PEG-amine is about 2-nm thick.

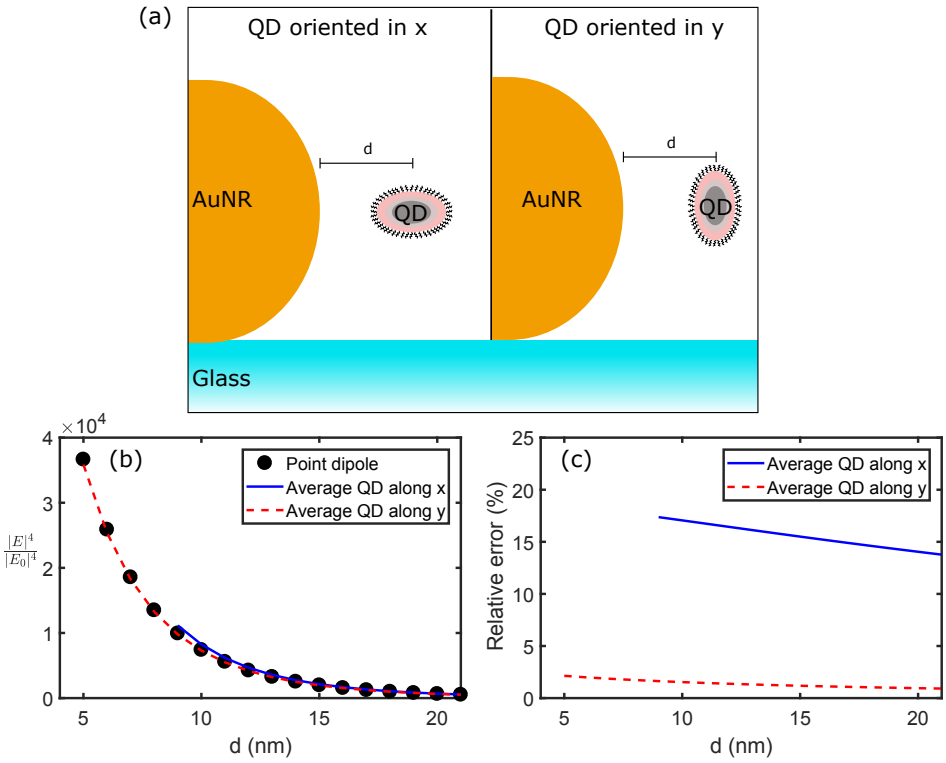


Figure S5.9: (a) Scheme of the average procedure. (b) Excitation enhancement for a point dipole and the averaged values for the two situations described on top. (c) Relative error

## 5.5.10. Effect of finite size of the quantum dot

In order to take into account the finite size of the QD we averaged the near-field map over the dimensions of the QD core. Figure S5.9(a) shows a scheme for the two situations taken into account: the quantum dot oriented along the longitudinal axis of the nanorod (x) and along the transverse axis (y). Figure S5.9(b) shows the resulting curves with the presented notation. The point dipole approximation gives rise to an error smaller than 20% in all cases.

## References

[1] K. Kneipp, H. Kneipp, I. Itzkan, R. R. Dasari, and M. S. Feld, *Ultrasensitive chemical analysis by raman spectroscopy,* Chemical Reviews **99**, 2957 (1999).

[2] J. F. Li, Y. F. Huang, Y. Ding, Z. L. Yang, S. B. Li, X. S. Zhou, F. R. Fan, W. Zhang, Z. Y. Zhou, D. Y. Wu, B. Ren, Z. L. Wang, and Z. Q. Tian, *Shell-isolated nanoparticle-enhanced raman spectroscopy,* Nature **464**, 392 (2010).

[3] R. Bardhan, N. K. Grady, J. R. Cole, A. Joshi, and N. J. Halas, *Fluorescence enhancement by au nanostructures: nanoshells and nanorods,* Acs Nano **3**, 744 (2009).

[4] O. L. Muskens, V. Giannini, J. A. Sanchez-Gil, and J. Gomez Rivas, *Strong enhancement of the radiative decay rate of emitters by single plasmonic nanoantennas,* Nano Letters **7**, 2871 (2007).

[5] F. Tam, G. P. Goodrich, B. R. Johnson, and N. J. Halas, *Plasmonic enhancement of molecular fluorescence,* Nano Letters **7**, 496 (2007).

[6] G. Boyd, T. Rasing, J. Leite, and Y. Shen, *Local-field enhancement on rough surfaces of metals, semimetals, and semiconductors with the use of optical second-harmonic generation,* Physical Review B **30**, 519 (1984).

[7] A. Bouhelier, M. Beversluis, A. Hartschuh, and L. Novotny, *Near-field second-harmonic generation induced by local field enhancement,* Physical Review Letters **90**, 013903 (2003).

[8] S. Khatua, P. M. R. Paulo, H. Yuan, A. Gupta, P. Zijlstra, and M. Orrit, *Resonant plasmonic enhancement of single-molecule fluorescence by individual gold nanorods,* ACS Nano **8**, 4440 (2014).

[9] X. Li, F.-J. Kao, C.-C. Chuang, and S. He, *Enhancing fluorescence of quantum dots by silica-coated gold nanorods under one- and two-photon excitation,* Optics Express **18**, 11335 (2010).

[10] Y. Fu, J. Zhang, and J. R. Lakowicz, *Plasmon-enhanced fluorescence from single fluorophores end-linked to gold nanorods,* Journal of the American Chemical Society **132**, 5540 (2010).

[11] Z. Yang, W. Ni, X. Kou, S. Zhang, Z. Sun, L.-D. Sun, J. Wang, and C.-H. Yan, *Incorporation of gold nanorods and their enhancement of fluorescence in mesostructured silica thin films,* The Journal of Physical Chemistry C **112**, 18895 (2008).

[12] J. N. Farahani, D. W. Pohl, H.-J. Eisler, and B. Hecht, *Single quantum dot coupled to a scanning optical antenna: a tunable superemitter,* Physical Review Letters **95**, 017402 (2005).

[13] A. Kinkhabwala, Z. Yu, S. Fan, Y. Avlasevich, K. Müllen, and W. Moerner, *Large single-molecule fluorescence enhancements produced by a bowtie nanoantenna,* Nature Photonics **3**, 654 (2009).

[14] H. Kano and S. Kawata, *Two-photon-excited fluorescence enhanced by a surface plasmon,* Optics Letters **21**, 1848 (1996).

[15] J.-M. Jung, H.-W. Yoo, F. Stellacci, and H.-T. Jung, *Two-photon excited fluorescence enhancement for ultrasensitive DNA detection on large-area gold nanopatterns,* Advanced Materials **22**, 2542 (2010).

[16] N. J. Greybush, M. Saboktakin, X. Ye, C. Della Giovampaola, S. J. Oh, N. E. Berry, N. Engheta, C. B. Murray, and C. R. Kagan, *Plasmon-enhanced upconversion luminescence in single nanophosphor–nanorod heterodimers formed through template-assisted self-assembly,* ACS Nano **8**, 9482 (2014).

[17] Y. Xue, C. Ding, Y. Rong, Q. Ma, C. Pan, E. Wu, B. Wu, and H. Zeng, *Tuning plasmonic enhancement of single nanocrystal upconversion luminescence by varying gold nanorod diameter,* Small **13** (2017).

[18] H. Yuan, S. Khatua, P. Zijlstra, M. Yorulmaz, and M. Orrit, *Thousand-fold enhancement of single-molecule fluorescence near a single gold nanorod,* Angewandte Chemie International Edition **52**, 1217 (2013).

[19] A. Samanta, Y. Zhou, S. Zou, H. Yan, and Y. Liu, *Fluorescence quenching of quantum dots by gold nanoparticles: a potential long range spectroscopic ruler,* Nano Letters **14**, 5052 (2014).



[20] W. Wenseleers, F. Stellacci, T. Meyer-Friedrichsen, T. Mangel, C. A. Bauer, S. J. Pond, S. R. Marder, and J. W. Perry, *Five orders-of-magnitude enhancement of two-photon absorption for dyes on silver nanoparticle fractal clusters,* The Journal of Physical Chemistry B **106**, 6853 (2002).

[21] I. Cohanoschi, S. Yao, K. D. Belfield, and F. E. Hernández, *Effect of the concentration of organic dyes on their surface plasmon enhanced two-photon absorption cross section using activated au nanoparticles,* Journal of Applied Physics **101**, 086112 (2007).

[22] S. T. Sivapalan, J. H. Vella, T. K. Yang, M. J. Dalton, R. N. Swiger, J. E. Haley, T. M. Cooper, A. M. Urbas, L.-S. Tan, and C. J. Murphy, *Plasmonic enhancement of the two photon absorption cross section of an organic chromophore using polyelectrolyte-coated gold nanorods,* Langmuir **28**, 9147 (2012).

[23] T. Zhao, K. Yu, L. Li, T. Zhang, Z. Guan, N. Gao, P. Yuan, S. Li, S. Q. Yao, Q.-H. Xu, and G. Q. Xu, *Gold nanorod enhanced two-photon excitation fluorescence of photosensitizers for two-photon imaging and photodynamic therapy,* ACS Applied Materials & Interfaces **6**, 2700 (2014).

[24] A. M. Craciun, M. Focsan, L. Gaina, and S. Astilean, *Enhanced one- and two-photon excited fluorescence of cationic (phenothiazinyl)vinyl-pyridinium chromophore attached to polyelectrolyte-coated gold nanorods,* Dyes and Pigments **136**, 24 (2017).

[25] S. T. Sivapalan, J. H. Vella, T. K. Yang, M. J. Dalton, J. E. Haley, T. M. Cooper, A. M. Urbas, L.-S. Tan, and C. J. Murphy, *Off-resonant two-photon absorption cross-section enhancement of an organic chromophore on gold nanorods,* The Journal of Physical Chemistry Letters **4**, 749 (2013).

[26] T. Zhang, G. Lu, J. Liu, H. Shen, P. Perriat, M. Martini, O. Tillement, and Q. Gong, *Strong two-photon fluorescence enhanced jointly by dipolar and quadrupolar modes of a single plasmonic nanostructure,* Applied Physics Letters **101**, 051109 (2012).

[27] S.-H. Gong, S. Kim, J.-H. Kim, J.-H. Cho, and Y.-H. Cho, *Site-selective, two-photon plasmonic nanofocusing on a single quantum dot for near-room-temperature operation,* ACS Photonics **5**, 711 (2018).

[28] A. B. Taylor, A. M. Siddiquee, and J. W. M. Chon, *Below melting point photothermal reshaping of single gold nanorods driven by surface diffusion,* ACS Nano **8**, 12071 (2014).

[29] P. Zijlstra, J. W. Chon, and M. Gu, *White light scattering spectroscopy and electron microscopy of laser induced melting in single gold nanorods,* Physical Chemistry Chemical Physics **11**, 5915 (2009).

[30] W. Albrecht, T.-S. Deng, B. Goris, M. A. van Huis, S. Bals, and A. van Blaaderen, *Single particle deformation and analysis of silica-coated gold nanorods before and after femtosecond laser pulse excitation,* Nano Letters **16**, 1818 (2016).

[31] S. Link and M. A. El-Sayed, *Spectral properties and relaxation dynamics of surface plasmon electronic oscillations in gold and silver nanodots and nanorods,* The Journal of Physical Chemistry B **103**, 8410 (1999).

[32] M. Yorulmaz, S. Khatua, P. Zijlstra, A. Gaiduk, and M. Orrit, *Luminescence quantum yield of single gold nanorods,* Nano Letters **12**, 4385 (2012).

[33] K. Zhang, H. Chang, A. Fu, A. P. Alivisatos, and H. Yang, *Continuous distribution of emission states from single cdse/zns quantum dots,* Nano Letters **6**, 843 (2006).

[34] C. B. Talbot, R. Patalay, I. Munro, S. Warren, F. Ratto, P. Matteini, R. Pini, H. G. Breunig, K. Konig, A. C. Chu, G. W. Stamp, M. A. Neil, P. M. French, and C. Dunsby, *Application of ultrafast gold luminescence to measuring the instrument response function for multispectral multiphoton fluorescence lifetime imaging,* Optics Express **19**, 13848 (2011).

[35] A. A. Kinkhabwala, Z. Yu, S. Fan, and W. E. Moerner, *Fluorescence correlation spectroscopy at high concentrations using gold bowtie nanoantennas,* Chemical Physics **406**, 3 (2012).

[36] S. Khatua, H. Yuan, and M. Orrit, *Enhanced-fluorescence correlation spectroscopy at micro-molar dye concentration around a single gold nanorod,* Physical Chemistry Chemical Physics **17**, 21127 (2015).

[37] C. Galland, Y. Ghosh, A. Steinbrück, M. Sykora, J. A. Hollingsworth, V. I. Klimov, and H. Htoon, *Two types of luminescence blinking revealed by spectroelectrochemistry of single quantum dots,* Nature **479**, 203 (2011).

[38] C. Galland, Y. Ghosh, A. Steinbrück, J. A. Hollingsworth, H. Htoon, and V. I. Klimov, *Lifetime blinking in nonblinking nanocrystal quantum dots,* Nature Communications **3**, 908 (2012).

[39] X. Ma, H. Tan, T. Kipp, and A. Mews, *Fluorescence enhancement, blinking suppression, and gray states of individual semiconductor nanocrystals close to gold nanoparticles,* Nano Letters **10**, 4166 (2010).

[40] S. J. LeBlanc, M. R. McClanahan, M. Jones, and P. J. Moyer, *Enhancement of multiphoton emission from single cdse quantum dots coupled to gold films,* Nano Letters **13**, 1662 (2013).

[41] J. Yao, D. R. Larson, H. D. Vishwasrao, W. R. Zipfel, and W. W. Webb, *Blinking and nonradiant dark fraction of water-soluble quantum dots in aqueous solution,* Proceedings of the National Academy of Sciences of the United States of America **102**, 14284 (2005).

[42] M. Caldarola, B. Pradhan, and M. Orrit, *Quantifying fluorescence enhancement for slowly diffusing single molecules in plasmonic near fields,* The Journal of Chemical Physics **148**, 123334 (2018).

[43] A. Biebricher, M. Sauer, and P. Tinnefeld, *Radiative and nonradiative rate fluctuations of single colloidal semiconductor nanocrystals,* The Journal of Physical Chemistry B **110**, 5174 (2006).

[44] N. Amecke and F. Cichos, *Intermediate intensity levels during the emission intermittency of single CdSe/ZnS quantum dots,* Journal of Luminescence **131**, 375 (2011).

[45] G. Schlegel, J. Bohnenberger, I. Potapova, and A. Mews, *Fluorescence decay time of single semiconductor nanocrystals,* Physical Review Letters **88**, 137401 (2002).

[46] B. R. Fisher, H.-J. Eisler, N. E. Stott, and M. G. Bawendi, *Emission intensity dependence and single-exponential behavior in single colloidal quantum dot fluorescence lifetimes,* The Journal of Physical Chemistry B **108**, 143 (2004).

[47] G. S. He, K.-T. Yong, Q. Zheng, Y. Sahoo, A. Baev, A. I. Ryasnyanskiy, and P. N. Prasad, *Multi-photon excitation properties of cdse quantum dots solutions and optical limiting behavior in infrared range,* Optics Express **15**, 12818 (2007).

[48] M. Marrocco, *Two-photon excitation fluorescence correlation spectroscopy of diffusion for gaussian- lorentzian volumes,* The Journal of Physical Chemistry A **112**, 3831 (2008).

[49] A. Nagy, J. Wu, and K. M. Berland, *Observation volumes and $\gamma$-factors in two-photon fluorescence fluctuation spectroscopy,* Biophysical Journal **89**, 2077 (2005).

[50] D. R. Larson, W. R. Zipfel, R. M. Williams, S. W. Clark, M. P. Bruchez, F. W. Wise, and W. W. Webb, *Water-soluble quantum dots for multiphoton fluorescence imaging in vivo,* Science **300**, 1434 (2003).

[51] E. Zamir, P. H. Lommerse, A. Kinkhabwala, H. E. Grecco, and P. I. Bastiaens, *Fluorescence fluctuations of quantum-dot sensors capture intracellular protein interaction dynamics,* Nature Methods **7**, 295 (2010).

[52] P. Sher, J. Smith, P. Dalgarno, R. Warburton, X. Chen, P. Dobson, S. Daniels, N. Pickett, and P. O'Brien, *Power law carrier dynamics in semiconductor nanocrystals at nanosecond timescales,* Applied Physics Letters **92**, 101111 (2008).

[53] P. B. Johnson and R.-W. Christy, *Optical constants of the noble metals,* Physical Review B **6**, 4370 (1972).

[54] M. T. Homer Reid and S. G. Johnson, *Efficient Computation of Power, Force, and Torque in BEM Scattering Calculations,* ArXiv e-prints (2013), arXiv:1307.2966 [physics.comp-ph] .

[55] `http://homerreid.com/scuff-EM`.

[56] L. Novotny and B. Hecht, *Principles of nano-optics* (Cambridge University Press, 2012).